05627-6-S

THE UNIVERSITY OF MICHIGAN

COLLEGE OF ENGINEERING
DEPARTMENT OF AEROSPACE ENGINEERING
HIGH ALTITUDE ENGINEERING LABORATORY

Scientific Report

The Scattering of Electromagnetic Waves From a Plasma-Immersed Cylinder

EDMUND K. MILLER

Under contract with:

National Aeronautics and Space Administration
Contract No. NASr-54(05)
Washington, D. C.

Administered through:

December 1966

OFFICE OF RESEARCH ADMINISTRATION • ANN ARBOR

THE UNIVERSITY OF MICHIGAN

COLLEGE OF ENGINEERING

Department of Aerospace Engineering

High Altitude Engineering Laboratory

Scientific Report

THE SCATTERING OF ELECTROMAGNETIC WAVES FROM A PLASMA-IMMERSED CYLINDER

Edmund K. Miller

ORA Project 05627

under contract with:

NATIONAL AERONAUTICS AND SPACE ADMINISTRATION

CONTRACT NO. NASr-54(05)

WASHINGTON, D. C.

administered through:

OFFICE OF RESEARCH ADMINISTRATION ANN ARBOR

December 1966

TABLE OF CONTENTS

LIST OF FIGURES

Abstract

The scattering cross-section of a perfectly conducting cylinder in a compressible plasma for incident transverse electric (TE) and transverse magnetic (TM) waves is theoretically investigated and numerical results are presented. The sheath which forms about an object in a plasma is represented in two ways, the first replacing the actual sheath by a free-space layer (the vacuum sheath) and the second taking into account the actual sheath inhomogeneity (the inhomogeneous sheath). It is found that only for near grazing incidence; for the electron plasma frequency near the incident wave frequency; or in the limit of small cylinder radii, are the TE-TE and TM-TM cross-sections appreciably affected by the plasma compressibility and sheath.

The Scattering of Electromagnetic Waves from a Plasma-Immersed Cylinder

I Introduction

There is currently a great deal of interest, in connection with radiation and scattering problems involving plasmas, to take into account the finite temperature of the plasma. This is because the warm plasma is compressible, and can support in addition to the electromagnetic (EM) wave, an electron acoustic wave. The coupling of this electron pressure wave, or as it will be referred to here, the electrokinetic (EK) wave, to the EM wave, may give rise to effects which cannot be explained by the usual cold plasma theory, where the plasma is characterized by an equivalent permittivity. One example of this is the scattering cross-section of a plasma cylinder, which exhibits resonances that can be accounted for only if the finite temperature of the plasma is taken into account.

It is natural to ask whether the finite plasma temperature will similarly have a perturbing effect on the scattering corss-section of an obstacle immersed in a plasma. For example, it may be shown (Wait, 1965) that the transverse electric (TE) polarization of the EM wave, upon scattering from a perfectly conducting, infinite cylinder in free space, produces only a scattered TE wave. The same is true for the incident transverse magnetic (TM) wave. The finite temperature of the plasma can alter this situation however, leading to conversion of TE to TM waves and TM to TE waves, as well as to scattered EK waves.

There is an additional mechanism which may lead to this polarization conversion, or cross-coupling as we will refer to it here, between the incident wave and the scattered fields. That is the sheath which

forms about a body in a plasma. (This sheath is of course a manifestation of the finite plasma temperature.) If the body is allowed to reach its floating potential in the plasma, as will be assumed here, the sheath is a region of electron deficiency, which may extend several electron Debye lengths into the plasma from the body. This is why, in dealing with EM waves in compressible plasmas, in many papers the sheath has been approximated by a free-space layer (the vacuum sheath) between the uniform plasma and the body. A more accurate representation of the sheath of course, would be one where the non-uniformity of the plasma within it is taken into account.

It is the purpose of this paper to investigate the effect of the plasma compressibility and sheath upon the scattering cross-section of an infinite, perfectly conducting cylinder, immersed in a plasma. The sheath will be represented in two ways, using the vacuum sheath model mentioned above, and a more realistic representation which takes the sheath inhomogeneity into account, the inhomogeneous sheath model. In both models, the sheath will be assumed to be of finite thickness, with the plasma external to the sheath uniform throughout. The theoretical development will be treated rather briefly, since the details have been presented elsewhere, in favor of giving the more interesting aspects of the numerical results in greater detail. A theoretical discussion in greater detail is given by Miller and Olte (1966a, 1966b).

II Formulation

The linearized hydrodynamic equations for the electrons (the ion motion is neglected), together with Maxwell's equations, serve to describe the time varying, or dynamic, field behavior in the plasma. It is assumed that there are no externally applied fields, and that collisional, viscous and gravitational force effects may be neglected. In the case of the vacuum sheath model expressions for each of the incident and scattered fields, both in the uniform plasma and vacuum sheath, are readily obtained in terms of Fourier series involving cylindrical Bessel functions and the unknown Fourier coefficients, which are to be obtained from the boundary conditions. For the inhomogeneous sheath model, solutions in the uniform plasma are similarly obtained, but the field equations for the sheath region require numerical integration. In either case, however, the scattering cross-sections, the quantities of interest here, are obtained from the Fourier coefficients for the scattered fields in the uniform plasma.

The Fourier coefficients for the fields produced by the incident wave are obtained from the boundary condition equations. The boundary conditions used for the vacuum sheath model are continuity of the tangential electric and magnetic fields at the sheath-plasma interface, vanishing of the tangential electric field on the cylinder, and either vanishing of the normal dynamic electron velocity (the hard boundary) or vanishing of the dynamic electron number density (the soft boundary) at the sheath-plasma interface. The latter boundary condition could be replaced by an admittance boundary condition relating the dynamic electron number density and velocity, where the surface admittance is arbitrary, but we have chosen to investigate only the extreme values of the range of possible admittance values. It is worthwhile to note,

that in the case of a soft boundary, there is no coupling between the EM and EK waves at the boundary, and thus no EM-EK coupling for the vacuum sheath model. Even in the case of the soft boundary however, there exists TE-TM and TM-TE coupling for a vacuum sheath of non-zero thickness.

The boundary conditions for the inhomogeneous sheath model are the same as those for the vacuum sheath above, with the exception that the normal dynamic electron velocity and dynamic electron number density be continuous at the sheath-uniform plasma interface. In addition, the boundary condition applied at the vacuum sheath-uniform plasma interface between the dynamic electron number density and velocity is now applied at the cylinder surface, since the plasma extends to the cylinder. In this case, the use of the soft boundary condition no longer means that the EM and EK waves are uncoupled, since the sheath inhomogeneity also produces coupling between them.

The differential scattering cross-section/unit length of the cylinder are then given by

$$\sigma^{D}_{--} = \frac{4\lambda_E^2}{K_E^3} \left| \sum_{n=-\infty}^{n=+\infty} e^{-in\varphi}\, i^n\, A^S_{n--} \right|^2 \qquad (1)$$

$$\sigma^{D}_{-p} = \frac{4}{N^2 K_E} \left| \sum_{n=-\infty}^{n=+\infty} e^{-in\varphi}\, i^n\, A^S_{n-p} \right|^2 \qquad (2)$$

where the first dash subscript on σ and the Fourier coefficient for the scattered field A^S, will be an e or m, denoting the incident wave to be either TE(E_z=0) or TM (H_z=0). The second dash subscript indicates the type of scattered wave, with p denoting the EK wave. The azimuthal angle φ is measured from the front of the cylinder as viewed by the incident plane wave. The other quantities are defined by

$$N=\omega_p/\omega=f_p/f$$

$$K_E=\frac{\omega}{v_\ell}\sqrt{1-N^2}=K_{Eo}\sqrt{1-N^2}$$

$$\lambda_E=K_E\sqrt{1-\cos^2\theta^i}$$

where f_p is the plasma frequency, f the incident wave frequency, v_ℓ is the velocity of light in free space and θ^i is the angle of incidence measured from the positive z-axis. Expressions for the A^s_{n--} are given by Miller (1966), for the vacuum sheath model. The scattering coefficients for the inhomogeneous sheath are obtained by numerical integration which is also discussed by Miller (1966)

The total scattering cross-sections are obtained by integrating (1), multiplied by $1/2\,\pi$, over ϕ from $-\pi$ to π with the result

$$\sigma^T_{--}=\frac{4\lambda_E^2}{K_E^3}\sum_{n=-\infty}^{n=\infty}\left|A_{n--}\right|^2 \qquad (3)$$

$$\sigma^T_{-p}=\frac{4}{N^2K_E}\sum_{n=-\infty}^{n=\infty}\left|A_{n-p}\right|^2 \qquad (4)$$

For purposes of investigating the conversion or coupling of TE to TM energy TM to TE energy, and EM to EK energy we define the coupling coefficients

$$C_{em}\equiv\sigma^T_{em}/\sigma^T_{ee} \qquad (5)$$

$$C_{me}\equiv\sigma^T_{me}/\sigma^T_{mm} \qquad (6)$$

$$C_{ep}\equiv\sigma^T_{ep}/\sigma^T_{ee} \qquad (7)$$

$$C_{mp}\equiv\sigma^T_{mp}/\sigma^T_{mm} \qquad (8)$$

The coupling coefficients thus represent the amount of energy scattered into fields of polarization different from that of the incident wave, in comparison with the scattered energy having the polarization of the incident wave. They should be useful in indicating the perturbing effect of the sheath and plasma compressibility on the scattering cross-section with the incident wave polarization. In the next section are presented numerical results for the cross-sections and coupling coefficients. For convenience, we will refer to σ^T_{ee} and σ^T_{mm} as the primary cross-sections, and will call the others conversion cross-sections in the following.

III. Numerical Results

There are a number of parameters which are of interest in connection with the effect their variation may have on the cross-sections and coupling coefficients. Perhaps the two most significant quantities which affect the coupling coefficients are the sheath thickness and electron temperature, since when both of these are zero, the coupling coefficients are also zero. Consequently, we present in Figs. 1 and 2 respectively, the variation of the 4 coupling coefficients with sheath thickness X and the electron temperature T, in ^{o}K. The sheath thickness X is in units of the electron Debye length (D_{ℓ}). The incident wave frequency in 1GHz, N = 0.7, $\theta^{i} = \pi/4$ and c = 5 cm.

There are curves plotted on Fig. 1 for results obtained from both the vacuum sheath model and the inhomogeneous sheath model for both the hard and soft boundaries. In the case of the inhomogeneous sheath, the static potential is taken to be of parabolic form, having the value -5.34 volts at the cylinder, corresponding to a mercury plasma with T = 10^{4} ^{o}K (see Miller and Olte, 1966b). Two curves are shown for each of the EM-EM coupling coefficients from the vacuum sheath model, one for the hard boundary and the other for the soft boundary, while the EM-EK coupling coefficients are shown of course for the hard boundary only. If we first observe the EM-EM coupling coefficients, we see that there is a rapid increase in the coupling coefficient with increasing vacuum sheath thickness, the increase being approximately $(X/2)^{2}$ referred to the X = 0 case, for the hard boundary. For the soft boundary (equivalent to a zero temperature plasma), the coupling coefficients are substantially the same as those for the hard boundary, for $X > 5$, but for thinner sheaths, there is a progressively increasing difference between the results for the two boundary conditions as X tends towards zero.

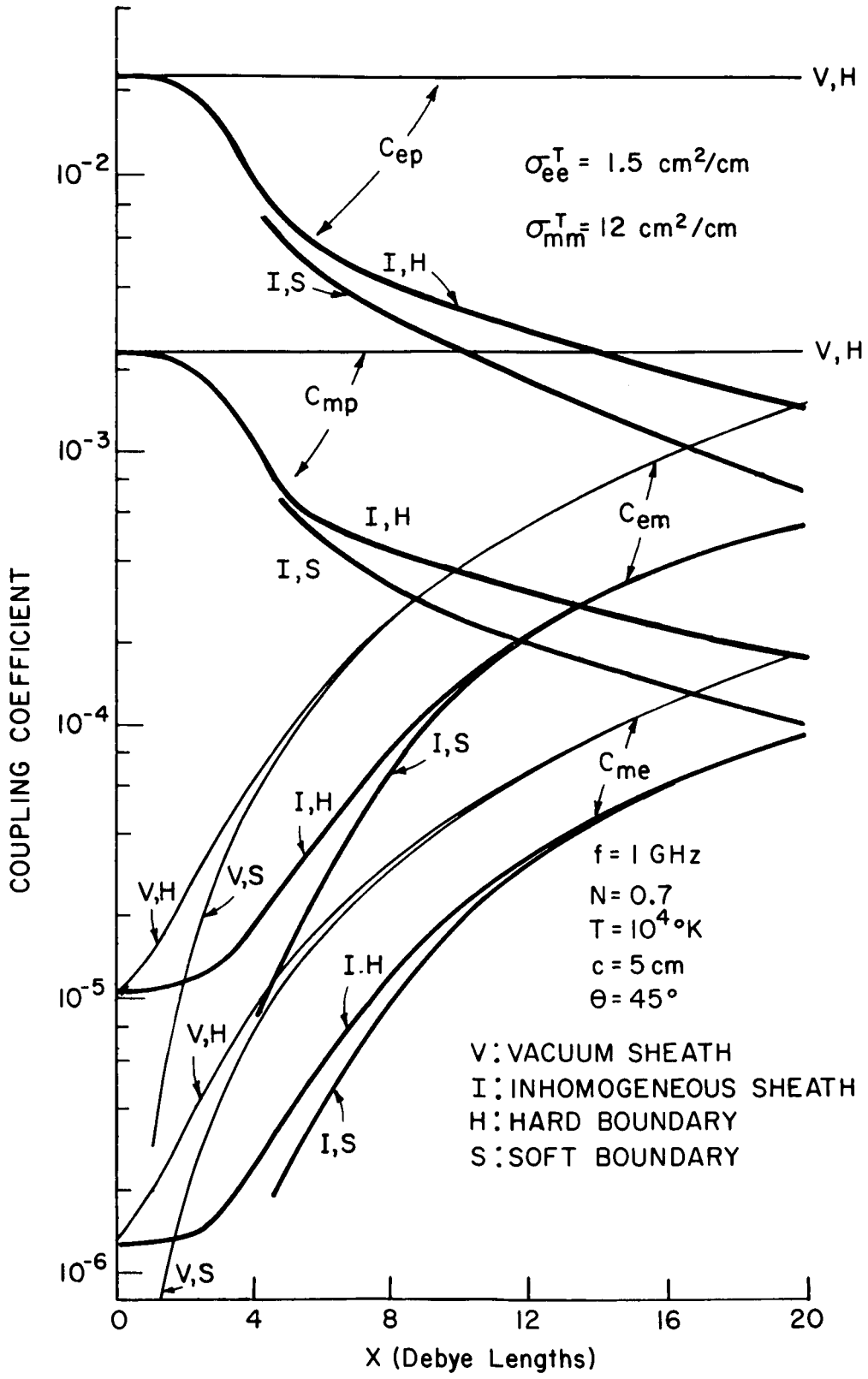

1. The coupling coefficients as a function of sheath thickness X for both the vacuum sheath and inhomogeneous sheath models and the soft and hard boundaries.

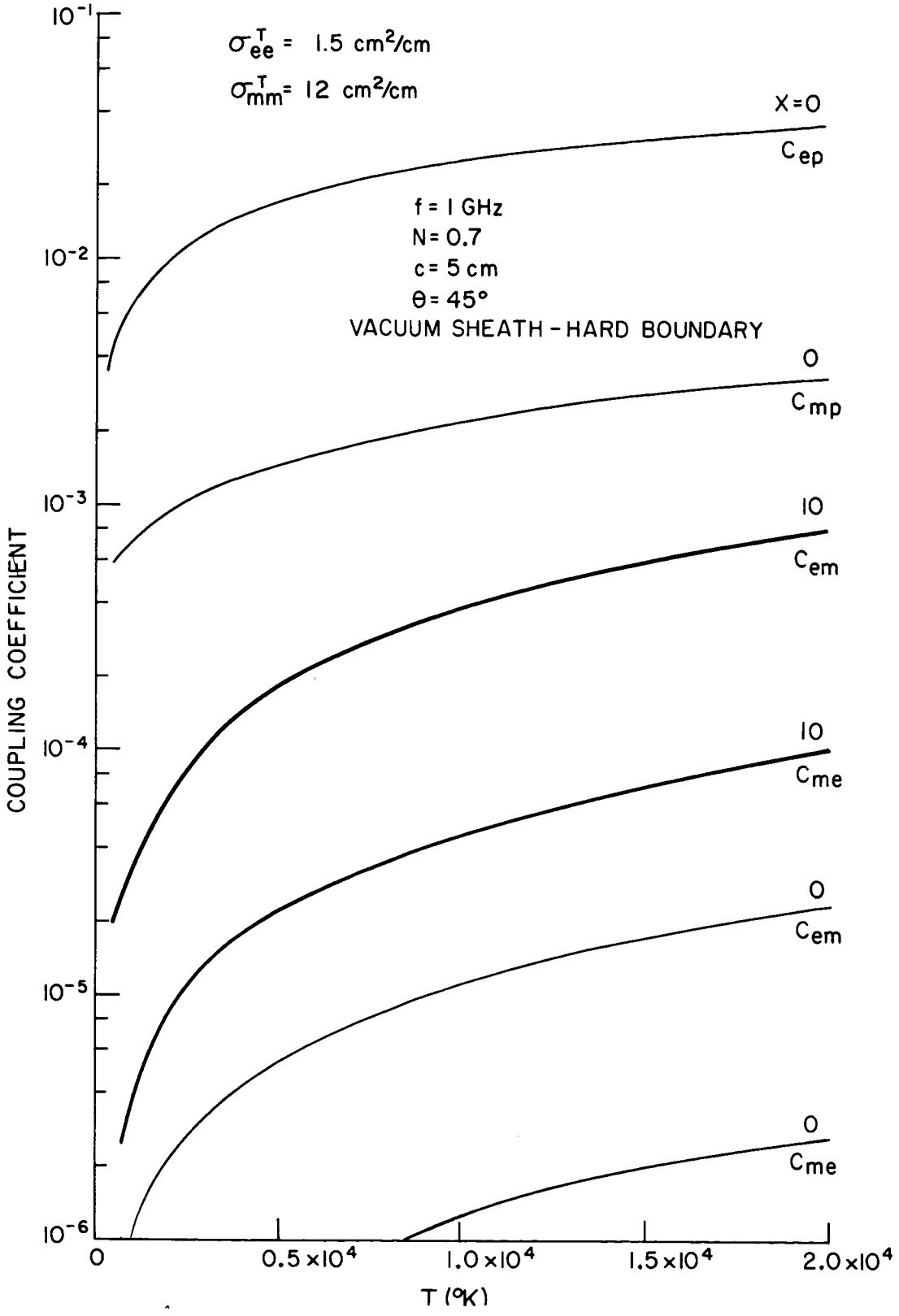

2. The coupling coefficients as a function of electron temperature T for the vacuum sheath model and the hard boundary.

The inhomogeneous sheath EM-EM coupling coefficients are seen to increase with increasing sheath thickness, in a way similar to the vacuum sheath results, for $X > 2$, and the hard boundary, with a vacuum sheath thickness approximately 0.6 the inhomogeneous sheath thickness leading to the same value for the coupling coefficient. In addition, the difference between the hard and soft boundary results for the inhomogeneous sheath is similar to that observed for the vacuum sheath for $X > 5$. For sheath thicknesses less than about 4 however, all the coupling coefficients exhibited an oscillatory behavior with decreasing X, for the soft boundary, sometimes becoming larger than the hard boundary results. Since the calculations required to accurately obtain this area of the curve would have been quite time consuming, this portion of the curves is not plotted.

When we turn our attention to the EM-EK coupling coefficients, we find that the vacuum sheath values are unaffected by changing sheath thickness, while the inhomogeneous sheath results show a generally decreasing coupling with increasing sheath thickness. As a result, near $X = 20$, the EM-EK coupling coefficients for the inhomogeneous sheath are on the same order of magnitude as the EM-EM coupling coefficients, while exceeding the EM-EM coupling coefficients by several orders of magnitude near $X = 0$. Contrary to the case of the EM-EM coupling coefficients, for $X > 5$, the hard boundary and soft boundary results for the EM-EK coupling coefficients and the inhomogeneous sheath diverge in value with increasing X.

It is of interest to note that neither σ_{ee}^{T} or σ_{mm}^{T} vary significantly from their sheathless value with changing X for both the vacuum sheath and inhomogeneous sheath models, the change being less than 1 per cent for X increasing from 0 to 20. Their sheathless values are $\sigma_{ee}^{T} = 1.5 \text{ cm}^2/\text{cm}$ and

σ^T_{mm} = 12 cm^2/cm, so that the conversion cross-sections can be obtained from Fig. 1 using equations (5) - (8).

Since the soft boundary results vary only slightly from the hard boundary results for X > 4 on Fig. 1, subsequent results are shown for the hard boundary only. In addition, since the inhomogeneous sheath and vacuum sheath results are similar, for the EM-EM coupling coefficients, the graphs to follow will be for the vacuum sheath model only. We note that the EM-EK coupling coefficients thus obtained from the vacuum sheath model will likely be somewhat exaggerated compared with values which would be obtained from the inhomogeneous sheath.

In Fig. 2., where the electron temperature is the dependent variable, results are given for the vacuum sheath model, and the hard boundary only, for X = 0 and 10. Note the absolute sheath thickness is now changing in proportion to the square root of the temperature, since $D_\ell = v_r/(\sqrt{3}\omega_p)$ where v_r is the rms electron velocity. Since there is no difference between the X = 0 and X = 10 case for C_{ep} and C_{mp}, only one curve is shown for each of these two quantities. It may be observed that the EM-EM coupling coefficients vary in proportion to the electron temperature T, while the EM-EK coupling coefficients vary as the square root of T. Again σ^T_{ee} and σ^T_{mm} were found to be nearly constant at their sheathless values, over the range of T shown, having the values given above.

The coupling coefficients are plotted as a function of θ^i, the angle of incidence, in Fig. 3, for the vacuum sheath model, and hard boundary, again for X = 0 and 10, with T = 10^4 ^oK and the other parameter values as for Fig. 1. We may observe that the coupling coefficients exhibit a decreasing trend as θ^i tends to normal incidence, and with the exception of C_{ep}, become zero at $\theta^i = \pi/2$.

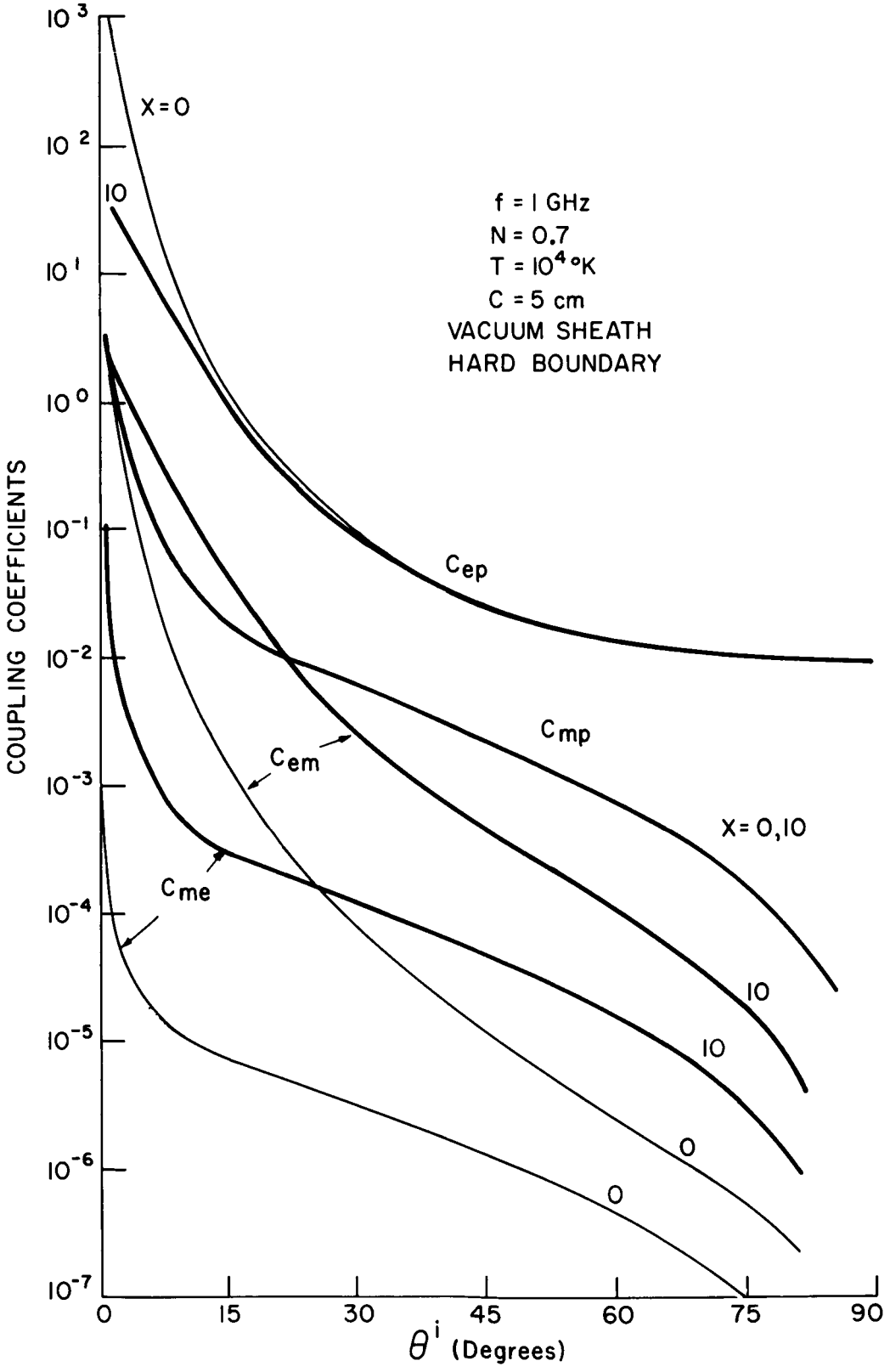

3. The coupling coefficients as a function of angle of incidence θ^i measured from the cylinder axis for the vacuum sheath model and the hard boundary.

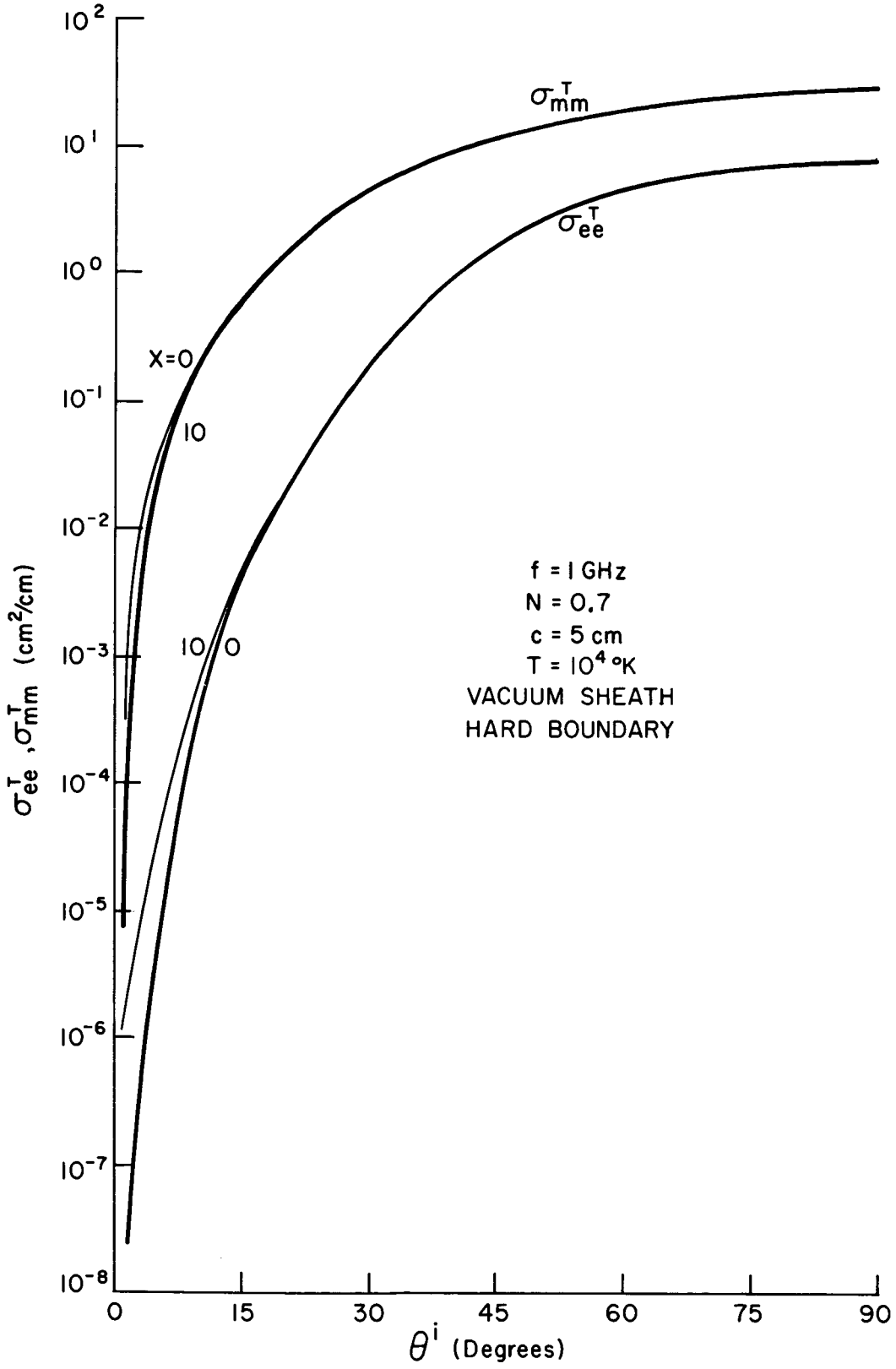

4. The primary cross-sections as a function of angle of incidence θ^i for the vacuum sheath model and the hard boundary.

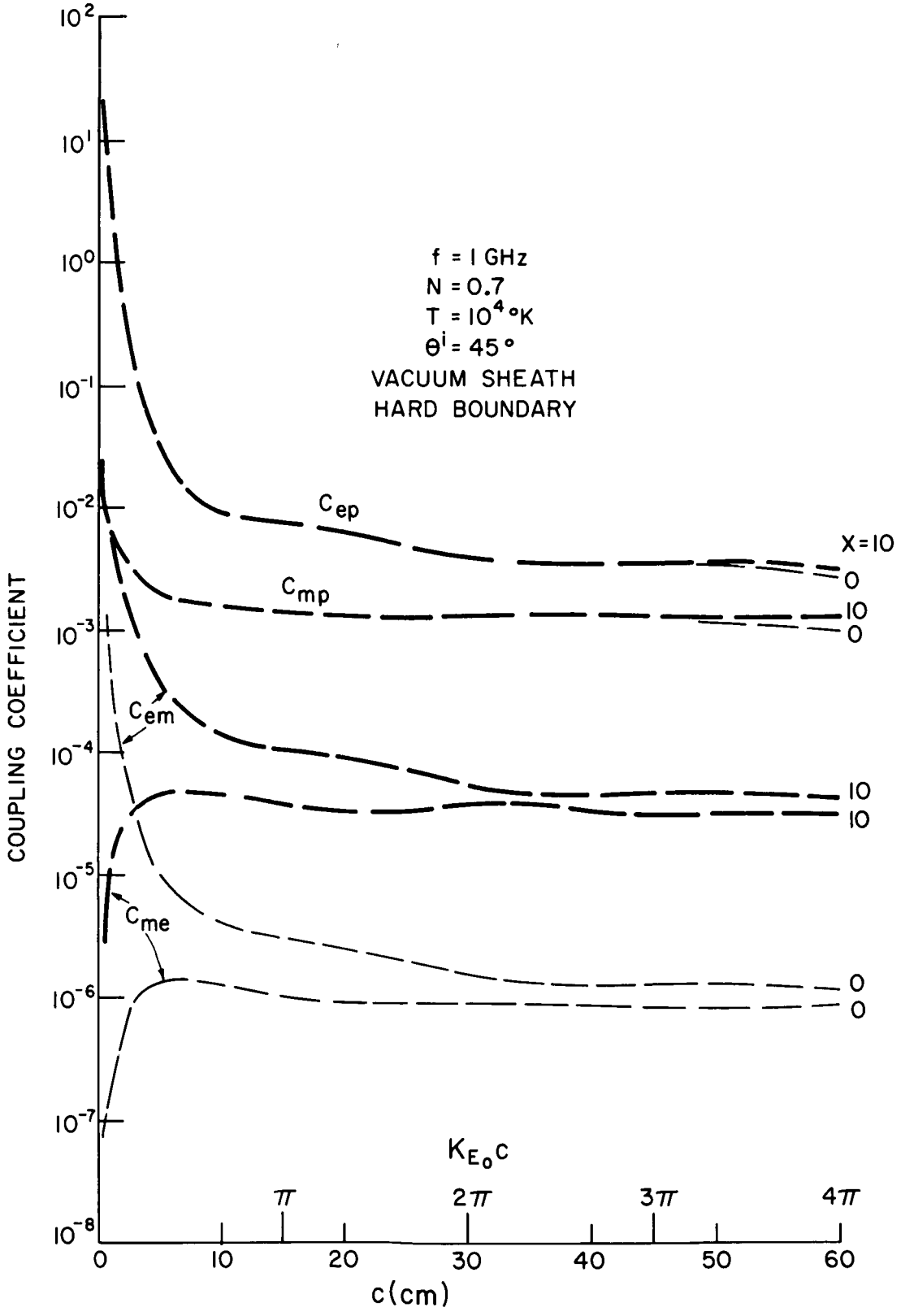

5. The coupling coefficients as a function of cylinder radius c for the vacuum sheath model and the hard boundary.

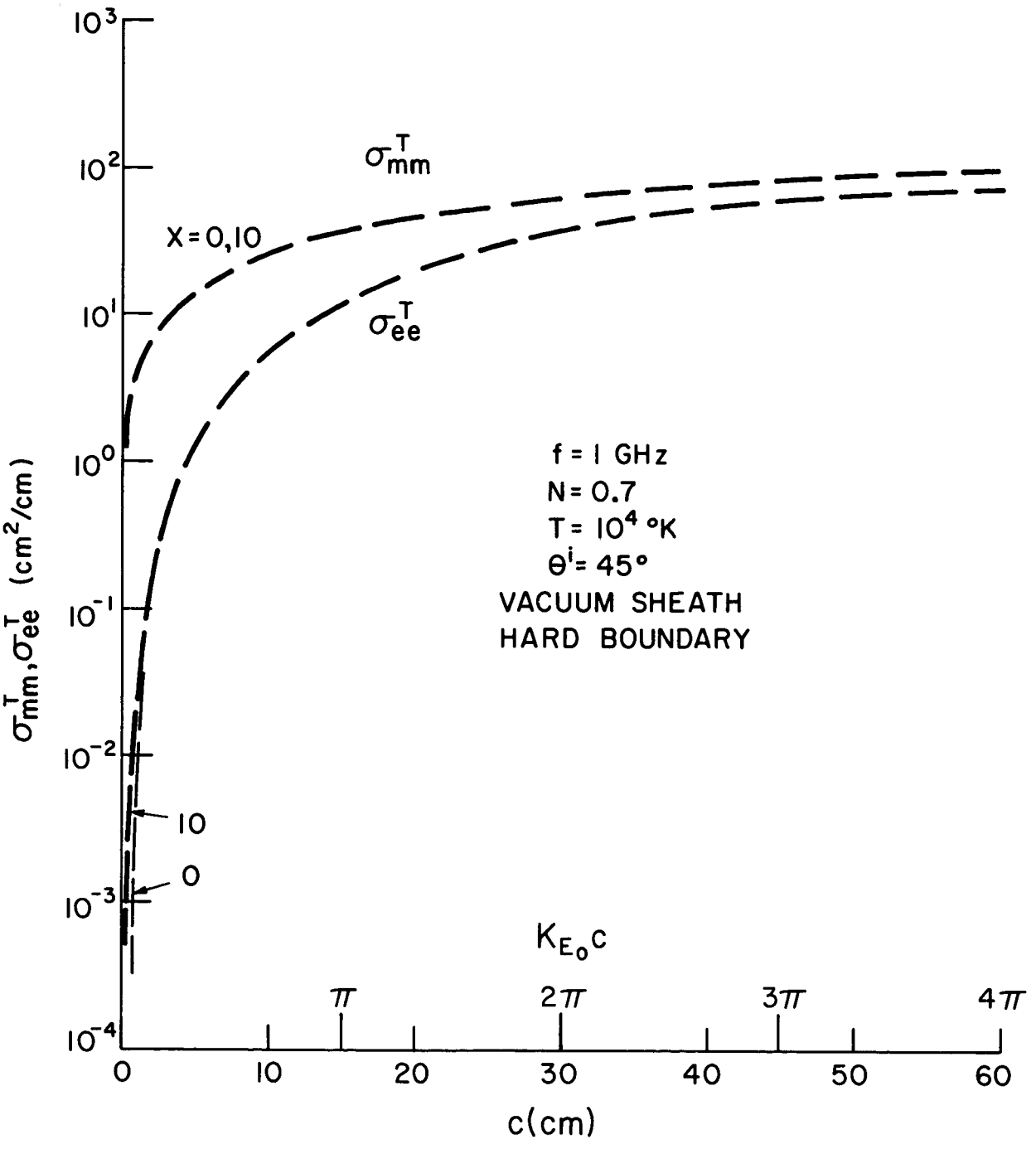

6. The primary cross-sections as a function of cylinder radius c for the vacuum sheath model and the hard boundary.

We may also see that the effect of the sheath is lessened for C_{em}, and remains unchanged for C_{me}, as θ^i tends towards zero. On the other hand, C_{ep} and C_{mp} begin to show a noticable sheath effect near grazing incidence. Because σ^T_{ee} and σ^T_{mm} vary with θ^i, these cross-sections are shown in Fig. 4. as a function of θ^i. It may be observed in Fig. 4 that the $10D_\ell$ thick vacuum sheath does influence the cross-section for near grazing angles of incidence, increasing σ^T_{ee} and decreasing σ^T_{mm} with respect to the sheathless case.

The cylinder radius c is the independent variable in Figs. 5 and 6, in which are shown respectively the coupling coefficients and the primary cross-sections σ^T_{ee} and σ^T_{mm} for the vacuum sheath model, and hard boundary for X = 0 and X = 10, with the other parameter values the same as for Fig. 1. The curves of Figs. 5 and 6 are drawn as dashed lines since the calculated points were not obtained close enough together to show the fine structure of the curves, but only to show the trend of the data with increasing cylinder radius c.

We see in Fig. 5 that the coupling coefficients show generally decreasing values with increasing cylinder radius. Since the TE wave decouples from the TM and EK waves for scattering from an infinite plane, we should expect that all the coupling coefficients except C_{mp} would become zero, if the radius c were given larger and larger values. The large increase in C_{ep}, C_{em} and C_{mp} as c approaches zero reflects the fact that the corresponding conversion cross-sections, while tending towards zero, do so more slowly then the primary cross-sections. It can be shown for example, that as $c \to 0$, $C_{ep} \to (v_\ell/v_r)^2/N^2$, from a small argument expansion of the scattering coefficients. This compares with $C_{ep} \to (v_\ell/v_r)^3/N^2$ for the scattering from a spherical plasma blob in the Rayleigh region, a result derived by Cohen (1962).

It is apparent that for large enough cylinder radii, C_{em} and C_{me} are approaching the same values, reflecting the fact that TM-TE and TE-TM coupling occurs with the same efficiency relative to the primary cross-sections. As a matter of interest, σ^T_{em} and σ^T_{me} are practically equal regardless of the cylinder radius, and sheath thickness, but for the smaller radii, σ^T_{ee} is less than σ^T_{mm}, producing a corresponding difference in the coupling coefficients C_{em} and C_{me}. We also observe in Fig. 5 that the effect of the sheath on the EM-EM coupling coefficients appearsto be independent of the cylinder radius, for the range investigated. The EM-EK coupling coefficients on the other hand, begin to exhibit a slight sheath dependence at the larger values of cylinder radii.

The final graphs of this series, Figs. 7 and 8, show respectively the coupling coefficients and the primary cross-sections σ^T_{ee} and σ^T_{mm} as functions of N, the ratio of f_p/f, with the other parameter values used for Fig. 1, and the vacuum sheath thicknesses of X=0 and X=10. We note that the TM-TE coupling coefficients of Fig. 7 and the TE-TE primary cross-section of Fig. 8 exhibit decreasing values with increasing N, while the converse behavior is true of the other coupling coefficients and the TM-TM primary cross-section. In addition, the sheath effect is observed to decrease with increasing N, a result to be expected since the sheath thickness relative to the wavelength is decreasing.

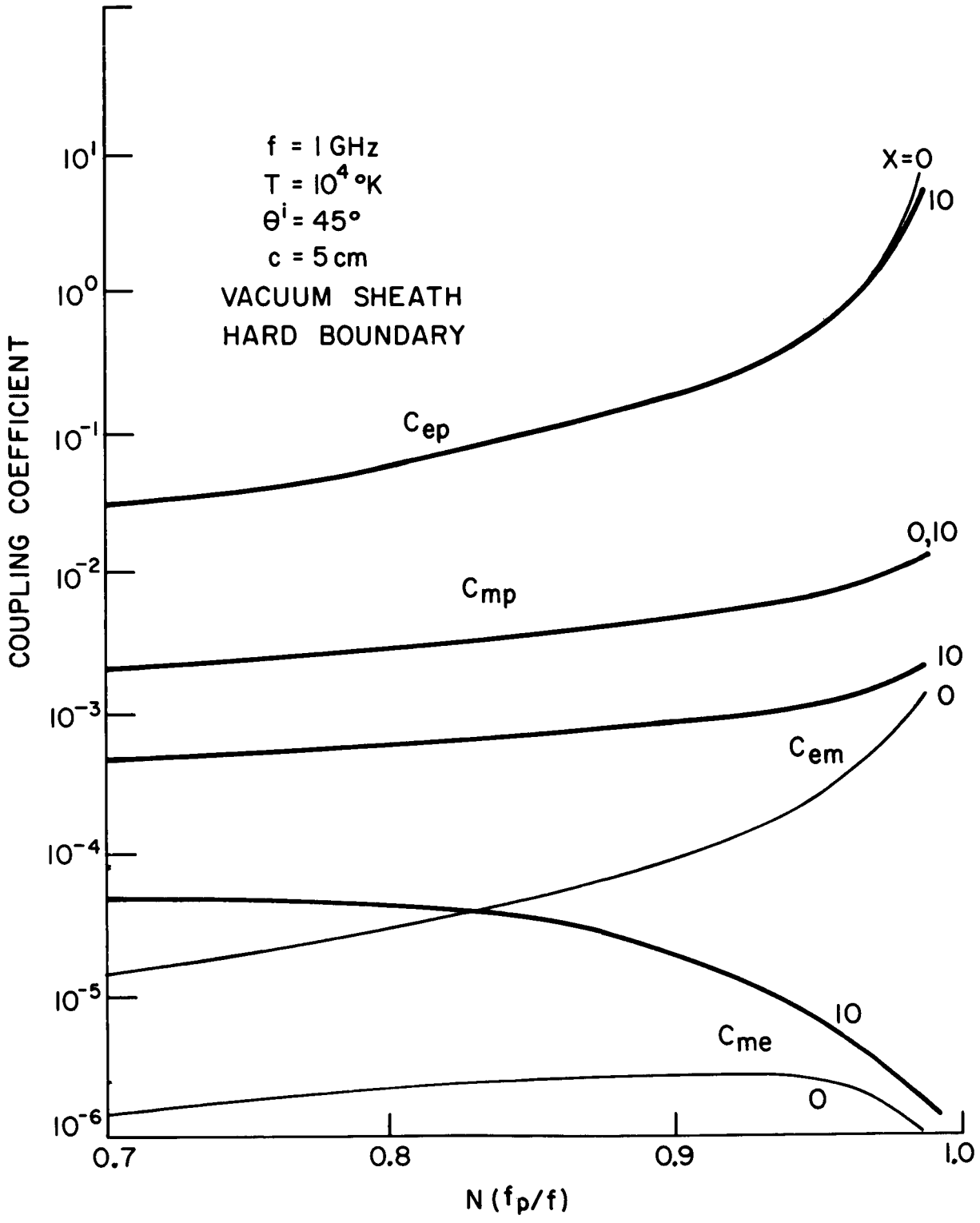

7. The coupling coefficients as a function of the plasma frequency to incident wave frequency ratio N, for the vacuum sheath model and hard boundary.

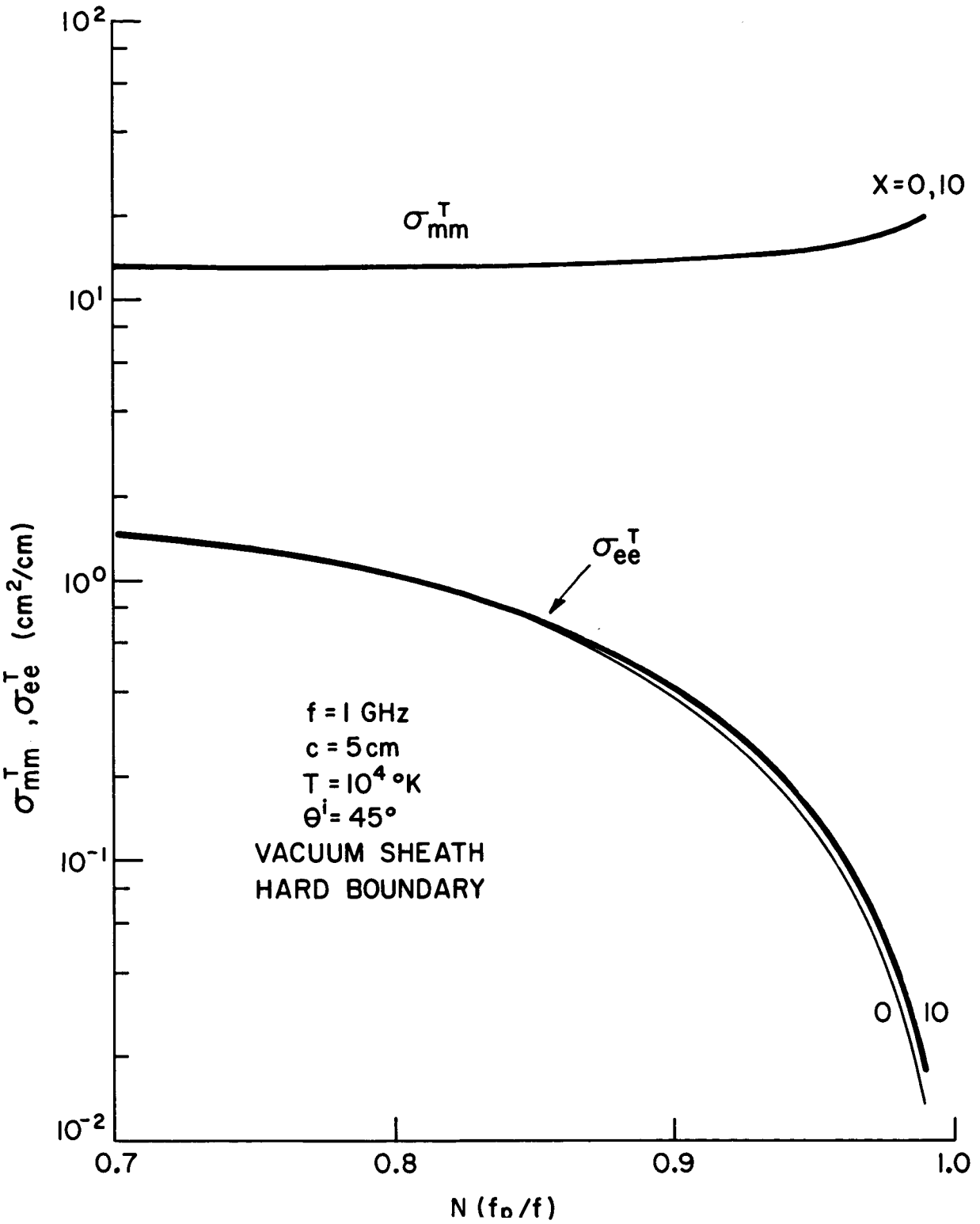

8. The primary cross-sections as a function of N for the vacuum sheath model and the hard boundary.

IV. Summary and Conclusion

The results of this investigation may be briefly summarized as follows:

(1) The primary cross-sections are negligibly affected by the plasma compressibility and sheath, except at near-grazing angles of incidence ($\theta^i < 15^o$), for N near unity or $K_{Eo}c << 1$, situations where the coupling coefficients approach unity.

(2) The EM-EM coupling coefficients increase approximately in proportion to the electron temperature and to the square of the vacuum sheath thickness expressed in electron Debye lengths. The EM-EK coupling coefficients vary as roughly the square root of the electron temperature and are practically unaffected by the vacuum sheath. The coupling coefficients are found to be less affected by the vacuum sheath as f_p/f approaches unity.

(3) With the exception of C_{ep}, the coupling coefficients are less than 10^{-2}, except for near grazing incidence, for N near unity or $K_{Eo}c << 1$.

(4) The inhomogeneous sheath primary cross-sections and EM-EM coupling coefficients are quantitatively similar to the vacuum sheath results, with a vacuum sheath approximately 0.6 the inhomogeneous sheath thickness (for the inhomogeneous sheath model used) producing coupling coefficients having the same values as the inhomogeneous sheath results. Only for the EM-EK coupling coefficients doe the vacuum and inhomogeneous sheath models differ appreciably, the inhomogeneous sheath results decreasing in magnitude while the vacuum sheath results remain constant, for increasing sheath thicknesses.

We can conclude from these results, as has been previously concluded by Miller and Olte (1966a, 1966b) in connection with the surface currents

excited on a plasma immersed cylinder by EM and EK waves, that the vacuum sheath approximates the inhomogeneous sheath quite well in predicting the scattering properties of the plasma immersed cylinder. An exception to this is the finding noted above that the EM-EK coupling is exaggerated by the vacuum sheath model as compared with the more realistic inhomogeneous sheath results.

We also conclude that while the sheath and plasma compressibility do lead to polarization conversion of the incident EM wave, the effect is small and has little influence on the primary scattering coefficients. In addition, the cross-coupled field components are generally orders of magnitude less than the primary scattered fields, and hence would probably be difficult to observe experimentally.

References

Cohen, M. H. (1962), "Radiation in a Plasma, II. Equivalent Sources", Phys. Rev., Vol. 126, No. 2, p 339-397.

Miller, E. K. (1966), "The Excitation of Surface Currents on a Plasma Immersed Cylinder by Electromagnetic and Electrokinetic Waves", to be published as aHigh Altitude Eng. Lab. report, U. of Mich. Ann Arbor, Mich.

Miller, E. K. and A. Olte (1966a), "Excitation of Surface Currents on a Plasma Immersed Cylinder by Electromagnetic and Electrokinetic Waves, I. The Vacuum Sheath". Radio Science, Vol. 1, No. 8, p 977-993.

Miller, E. K. and A. Olte (1966b), "Excitation of Surface Currents on a Plasma Immersed Cylinder by Electromagnetic and Electrokinetic Waves, II. The Inhomogeneous Sheath", to be published in December issue of Radio Science.

Wait, J. R. (1965), "Scattering of Electromagnetic and Electroacoustic Waves by a Cylindrical Object in a Compressible Plasma", Radio Science J. Res. NBS, Vol. 69D, No. 2, p 247-256.